文章编号 1004-924X(2009)06-1467-06

光镊驱动微转子

翟晓敏,黄文浩
(中国科学技术大学 精密机械与精密仪器系,安徽 合肥 230027)

摘要:光镊技术已经成功应用于光学和微功能器件,但是,对光镊驱动复杂微转子所建模型尚不成熟。为了分析光镊的光驱动力和力矩,基于矩量法建立了一种新模型。基于此种模型的分析结果表明改变环境参量是提高光镊工作效率的方法之一,如微转子转动速率与光镊的激光功率成正比,与束腰半径成非线性关系。另一种可以大幅度提高光镊工作效率的方法是改变微转子的形状,数据表明"万字"形微转子的转动效率是相同尺寸的"十字"形转子转动效率的 10^{-7} 倍。此外,通过解析力场的分布状态,可得到光压力的主要作用面,为今后的微转子设计提供依据。新模型的另一个优点是耗费时间较少,对于模拟光镊驱动微功能器件具有通用性和柔性。

关 键 词:微转子;矩量法;光镊
中图分类号:TM359.5;Q63 **文献标识码**:A

Driving microrotor by using optical tweezers

ZHAI Xiao-min, HUANG Wen-hao

(*Department of Precision Machinery and Precision Instrumentation, University of Science and Technology of China, Hefei* 230027, *China*)

Abstract: Optical tweezers have been successfully used in various scientific and engineering fields such as optics and microactuators. However, there is still a lack of a sophisticated model for optical tweezers on driving complex microrotors. In this paper, a novel model for optical tweezers is presented to calculate the optical force and torque based on the moment method. A numerical simulation of this model shows that one of the methods to improve the efficiency of an optical tweezer is to change variant conditions, such as the microrotor's speed is in proportion to the laser's power and has a nonlinear relation with the beam's waist. The other method to improve the efficiency for the optical tweezer is to change the microrotor's configuration. The results show that rotor speed of the microrotor is about 10^{-7} as large as that of the cross-shaped rotor. Furthermore, through analyzing the force placement, it is convenient to find the main surfaces that the optical forces act on, which can provide a foundation for the design of microrotors in the future. This model also has advantages in flexibility and universality in the optical force simulation of microactuators.

Key words: microrotor; moment method; optical tweezer

Received date: 2009-01-20; **Revised date**: 2009-04-30.

Foundation item: Supported by the National High-Tech Research and Development Program (863 Program) (Grant No. 2006AA04Z311)

1 Introduction

Optical tweezers are tools that use optical pressure in trapping, translating, and manipulating microscopic particles such as the living cells, the microorganisms and the artificial microactuators which are fabricated by micromachining[1-3]. The microrotor, which is an important sort of the micro－actuators, has been successfully driven by optical tweezers experimentally[4]. This is expected to solve the problems of an MEMS motor, i. e., short lifetime due to friction and requirement of electrical wires for the power supply. If the microrotor is a function device in a micro electromechanical system, it should be designed to meet some different requirements such as the geometrical characteristic, the power output and so on. In order to short the time of design and raise the probability of success, it is important to find a novel model for optical tweezers on driving complex microrotors. In this paper, the moment method is adopted to analyze the optical force and the optical torques which are acting on the microrotor.

2 Methodology

The laser beam with a wavelength λ is scattered by an arbitrarily shaped and homogeneous object whose permittivity is ε_2 and permeability is μ_2. The object is immersed in the medium whose permittivity is ε_1 and permeability is μ_1. Let J denotes the equivalent electric current on the object's surface and M denotes the magnetic ones. (E^1, H^1) denotes the incident fields. The electromagnetic field of the object is described by the Poggio-Miller-Chang-Harrington-Wu (PMCHW)[5] formulation.

$$Z_2 L_2(-J) - K_2(-M) - Z_1 L_1(J) + K_1(M) = E^1, \quad (1)$$

$$L_2(-M)/Z_2 + K_2(-J) - L_1(M)/Z_1 + K_1(J) = H^1. \quad (2)$$

where the operators L_1 and K_1 are defined as:

$$\begin{cases} L_1(X) = -\int K_1 \int [X + (1/K_1^2)\nabla(\nabla \cdot X)] G_1 \, d\tau \\ K_f(X) = -\int X \times \nabla G_1 \, d\tau \\ K_1 = \omega\sqrt{\mu_1 \varepsilon_1} = 2\pi/\lambda, G_1(r, r') = e^{jK_1|R|}/(4\pi|R|) \end{cases}, \quad (3)$$

$R = r - r'$, $(i = 1, 2)$. r is the location of the source point, and r' is the location of the field point. (Fig. 1)

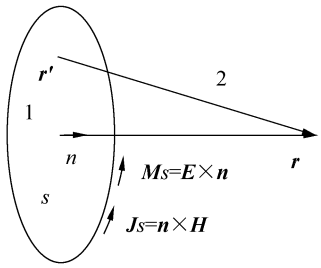

Fig. 1 Schematic of problem

In order to transform the integral equation (1) and (2) into matrix equations, the surface S is replaced by a triangular－patch model and the unknown effective electric and magnetic current J and M are expanded in vector basis functions associated with the edges of the triangulated surface.

$$J = \sum_{i=2}^{N_2} J_1 g_1, M = \sum_{i=1}^{N_2} M_1 g_1, \quad (4)$$

where N_2 denotes the total number of edges on S and $g_1 = (l_1/2\Delta)\rho_1$ denotes the RWG vector (Fig. 2) basis function, l_1 is the length of the edge i, Δ is the area of the triangle.

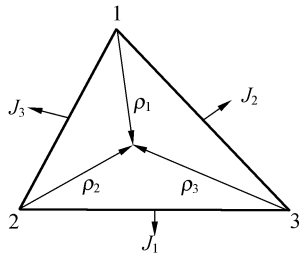

Fig. 2 RWG vector

Choose $\hat{n}/g_1$ as the testing function, $\hat{n}$ is the outward unit vector normal to S. For the PMCHW formulation, one takes the dot product of both sides of the equations with the testing function.

The moment method matrix equations for the unknown coefficients J and M can be written as:

$$\begin{bmatrix} P_1^{NF} & Q_1^{NF} \\ P_2^{NP} & Q_2^{NF} \end{bmatrix} \begin{pmatrix} J \\ M \end{pmatrix} = \begin{pmatrix} b_1^{NF} \\ b_2^{NF} \end{pmatrix} , \quad (5)$$

Where,

$$P_{1ij}^{NP} = -\int_S \hat{n} \times g_1 \cdot [Z_2 L_2(g_1) + Z_2 L_2(g_1)] \mathrm{d}S , \quad (6)$$

$$Q_{1ij}^{NP} = \int_S \hat{n} \times g_1 \cdot [K_2(g_1) + K_2(g_1)] \mathrm{d}S , \quad (7)$$

$$P_{2ij}^{NP} = -\int_S \hat{n} \times g_1 \cdot [K_2(g_1) + K_2(g_1)] \mathrm{d}S , \quad (8)$$

$$Q_{2ij}^{NP} = -\int_S \hat{n} \times g_1 \cdot [L_2(g_1)/Z_2 + L_2(g_1)/Z_2] \mathrm{d}S , \quad (9)$$

$$b_{1i}^{NP} = \int_S \hat{n} \times g_1 \cdot E^1 \mathrm{d}S, b_{2i}^{NP} = \int_S \hat{n} \times g_1 \cdot H^1 \mathrm{d}S . \quad (10)$$

Once the elements of the moment matrix and the excitation vector determined, one may solve the resulting system of linear equation (5) for the unknown coefficients J and M, and the scattered electric and magnetic field can be computed from the surface electric and the magnetic current. At each cell on the surface, Maxwell's stress tensor is used to estimate the instantaneous force exerted on the rotor,

$$\mathrm{d}\boldsymbol{F} = (\tilde{\boldsymbol{T}} \cdot \hat{\boldsymbol{n}}) \mathrm{d}S . \quad (11)$$

where,

$$T_{ij} = \varepsilon E_1 E_j + \mu H_1 H_j - b_{ij} (\varepsilon E^2 + \mu H^2)/2 . \quad (12)$$

3 Results and discussion

The moment method obtains the electromagnetic field through dispersing the object into many small cells and calculating the effect between each unit. However complex the trapped object's figure is, it is easy to gain the trapping force based on the moment method. Our laboratory had built a microrotor and driven it by a single beam optical tweezers. The microrotor's geometry is shown in Fig. 3.

The microrotor's rotation speed reached at two hundred rings per minute when it is controlled by the laser with a wavelength of 808nm and focused in the sample area by a high-numerical-aperture objective lens (oil immersion 100/1.25). The power of the laser beam is about 50

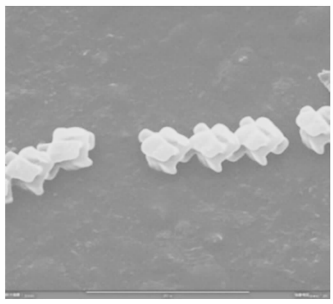

(a) SEM picture of microrotors

(b) Microscopical view of untrapped microrotor

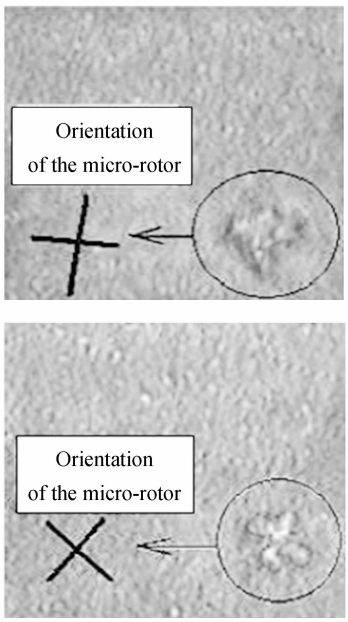

(c) Two microscopical views of different positions of microrotor in rotation

Fig. 3 Geometry sketches of microrotor

mW. The refractive index of the microrotor is $n_2 = 1.47$, and it is immersed in the acetone ($n_1 = 1.36$). The microrotor's surface is dived into the triangular cells, as shown in Fig. 4(b), and a quarter of the object has been designed and the sencond plane is located in the *XOY* plane. The microrotor's thickness is about 5 μm.

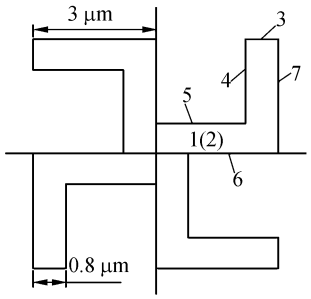

(a) Planform of microrotor 1

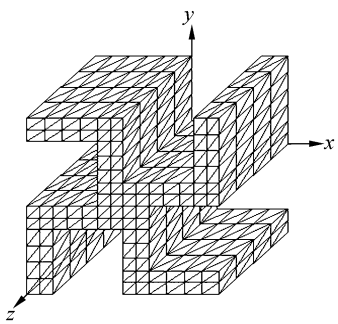

(b) Triangular representation of its surface for the microrotor

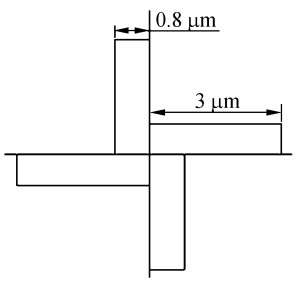

(c) Geometry of microrotor 2

Fig. 4 Microrotors

When the microrotor is trapped by a laser beam which is propagating in the Z axis direction, the force and torque on its surface can be gained according to the method which is mentioned in the part 2. The angular velocity is exhibited in the Fig. 5(a) as a function of the laser power, and it is linearly dependent on the beam energy. So we can improve the rotation rate by adjusting the incident beam power. But if the incidental energy is too high, the microrotor may be destroyed by the laser.

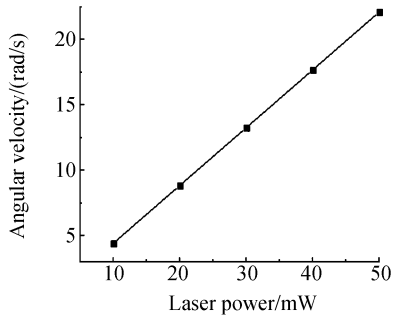

(a) Rotational speed applied to the motor *vs* laser intensity

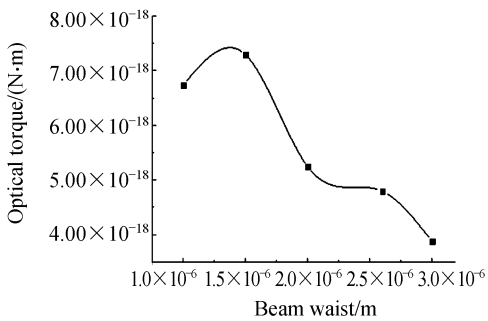

(b) Torque applied to the first micromotor *vs* beam waist

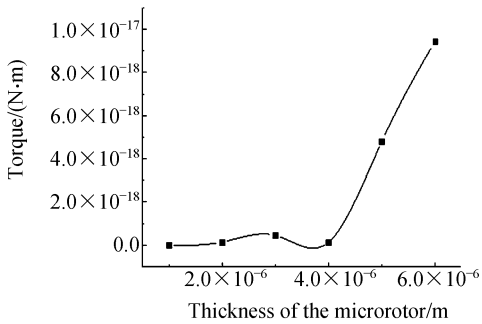

(c) Torque applied to the first micromotor *vs* its thickness

Fig. 5 Plots of optical torque and rotational speed as functions of laser power, beam waist and microrotor's thickness

Fig. 5(b) (c) shows the optical torque, T, plotted as a function of the beam waist. The optical torque is decreasing when the laser beam waist is increasing. The reason which causes this phenomenon is mainly the momentum changes that is happening at the plane 4,7 in the scattering process. Another important evidence to sustain the explanation is that we had built a similar microrotor whose geometry is shown in Fig. 4 (c). We tried to drive it by using the single beam optical tweezers but it failed, and then the model which is mentioned in the part 2 had been used to analyze the second microrotor. The numerical calculation results which are shown in the table one express that the torque acting on the second microrotor is about seventh smaller than the first one. This torque is too small. It can thus be concluded that the optical forces are mainly forced on the epitaxial arms of the first microrotor.

Tab. 1 Optical torqures for two microrotors with various laser powers

laser power	30 mW	40 mW	50 mW
torque of the first microrotor ($\times10^{-18}$ N·m)	2.876 2	3.834 7	4.793 0
torque of the second microrotor ($\times10^{-25}$ N·m)	2.420 6	3.227 5	4.034 5

Dependences of the optical torque upon the thickness of the microrotor are shown as Fig. 5 (c). It is obvious that the higher the microrotor is, the faster it can rotate for a fixed laser power. The reason which cause this phenomenon is mainly that the scattering power is enhanced when the thickness of the microrotor increases. Another important reason why this is an effective way to improve the rotor frequency is that the epitaxial arms of force are comparative longer than the internal arms'.

4 Conclusion

In this paper the moment method for optical tweezers was presented, which can be used to determine the radiation pressure forces and torques on the complex microactuators. Some influencing factors of the optical trapping efficiency have been discussed by using this theoretical model. To our knowledge, it is the first time to apply the moment method in optical trapping force calculations. By using this model, it is easy to analyze the force placement of the microrotors and find an effective way to improve the rotor frequency. Another important advantage of the moment method is less time-consuming comparing to other methods. It only takes about 120 min to finish the whole calculation of the model in this paper (a compute with Core 2 Duo CPU E6550@2.33GHz 2.33GHz and 2G memory). Furthermore, the fast multipole method could be used to decrease the time-consuming if the object has large leading dimensions or complex outline which can lead to increase the time spent in computing the coefficient matrix. The algorithm presented here can be easily extended to another complex objects' optical force calculation, thus providing a highly flexible and universally useable computation engine in the simulations about the optical tweezers.

References:

[1] ASHKIN A, DZIEDZIC J M. Optical levitation by radiation pressure[J]. *Appl. Phys. Lett.*, 1971, 19 (18): 283-284.

[2] GRAHAM D W, JOCHEN A, WILSON C K P, *et al*.. Experimentally anipulating fungi with optical tweezers[J]. *The Mycological Society of Japan and Springer*, 2007, 48: 15-19.

[3] YAO X CH, LI ZH L, GUO H L, *et al*.. Optical trap steering system[J]. *Opt. Precision Eng.*, 2001, 9(1): 55-58. (in Chinese)

[4] PÉTER G, PÁL O. Complex micromachines produced and driven by light[J]. *Applied Physics Letters*, 2001, 78: 249-251.

[5] MAUTZ J R, HARRINGTON R F. Electromagnetic scattering from a homogeneous material body of revolution[J]. *AEU, Electron. Commun.*, 1979, 33: 71 - 80.

Authors' biographies:

ZHAI Xiao-min (1982—), female, Ph. D. candidate of the University of Science and Technology of China, her researches focus on optical tweezers, MEMS devices, lithography technology, microsystem and so on. **E-mail**: xmzhai@mail.ustc.edu.cn

HUANG Wen-hao (1944—), male, professor of the University of Science and Technology of China, his researches focus on AFM, femtosecond laser two-photo 3D microfabrication technology, three-dimensional optical data storage and so on. **E-mail**: whuang@ustc.edu.cn

●下期预告

基于聚类和分形的复杂背景下扩展目标分割

张坤华, 杨 烜

(深圳大学 信息工程学院, 广东 深圳 518060)

将 K-均值聚类方法与分形理论相结合, 提出了一种新的两阶段扩展目标分割的方法。在预分割阶段, 首先运用粗糙集理论求取初始聚类中心, 在 K-均值聚类分割和区域连通的基础上, 检测图像边缘并进行边界跟踪, 对于获得的目标和背景团块根据扩展目标特性确定目标潜在区域。在进一步分割阶段, 给出图像分维数随尺度变化的函数, 利用自适应阈值, 根据分形理论的尺度不变性进一步抑制预分割结果中的自然背景, 并运用形态学开运算消除背景粘连。实验表明该方法能有效并可靠地实现复杂背景下扩展目标的精确分割, 分割出的扩展目标轮廓细节保持良好。